Biosensors and Bioelectronics 124–125 (2019) 143–149

Contents lists available at ScienceDirect

Biosensors and Bioelectronics

journal homepage: www.elsevier.com/locate/bios

# A microfluidic colorimetric biosensor for rapid detection of *Escherichia coli* O157:H7 using gold nanoparticle aggregation and smart phone imaging

Lingyan Zheng[a], Gaozhe Cai[b], Siyuan Wang[a], Ming Liao[c], Yanbin Li[d], Jianhan Lin[a,b,*]

[a] Key Laboratory of Agricultural Information Acquisition Technology, Ministry of Agriculture, China Agricultural University, Beijing 100083, China
[b] Key Laboratory of Modern Precision Agriculture System Integration Research, Ministry of Education, China Agricultural University, Beijing 100083, China
[c] College of Veterinary Medicine, South China Agricultural University, Guangzhou 510642, China
[d] Department of Biological and Agricultural Engineering, University of Arkansas, Fayetteville, AR 72701, United States

ARTICLE INFO

*Keywords:*
Colorimetric biosensor
Gold nanoparticle aggregation
Smart phone imaging APP
Microfluidic chip
*E. coli* O157:H7

ABSTRACT

We intended to develop a novel biosensor using gold nanoparticles (AuNPs) for indicating different concentrations of *E. coli* O157:H7 and smart phone imaging APP for monitoring color change of the AuNPs. The magnetic nanoparticles (MNPs) modified with the capture antibodies and the polystyrene microspheres (PSs) modified with the detection antibodies and the catalases were simultaneously used to react with the target bacteria in the first mixing channel of the microfluidic chip, and hydrogen peroxide was injected and catalyzed by the catalases on the MNP-bacteria-PS complexes. After the mixture of the AuNPs and the crosslinking agents were injected to react with the catalysate in the second mixing channel and incubated in the detection chamber, the aggregation of the AuNPs was triggered through the crosslinking agents, resulting in the color of the AuNPs changing from blue to red. Finally, the color was measured using the smart phone imaging APP to determine the amount of the bacteria. This biosensor exhibited a good specificity and sensitivity for detection of *E. coli* O157:H7 in chicken samples with a lower detection limit of 50 CFU/mL.

## 1. Introduction

Food safety has attracted increasing concerns globally (King et al., 2017; Omari et al., 2018). Foodborne illnesses are mainly caused by 15 pathogenic bacteria through the consumption of contaminated foods (Chen and Park, 2017a). *E. coli* O157:H7 is one of the major foodborne pathogenic bacteria and can often result in such serious diseases as hemolytic uremic syndrome, bloody diarrhea and even death (Jiang et al., 2016b; Zeinhom et al., 2018b). Existing methods for detection of *E. coli* O157:H7 mainly include culture plating (Culture), polymerase chain reaction (PCR), and enzyme-linked immune-sorbent assay (ELISA), etc. Culture is the gold standard method with high reliability and sensitivity, however it is time-consuming and generally needs 2–3 d. PCR is recommended in China's food safety national standards with short time and high sensitivity, however it often requires well-trained technicians and complex DNA extraction procedure (Wu et al., 2015). ELISA is featured with rapid detection and high throughput , however it lacks sufficient sensitivity and often has a low detection limit of $10^4$ CFU /mL (Feng et al., 2013; Wu et al., 2015). Therefore, it is crucial to develop simple, sensitive and rapid methods for bacteria detection to ensure food safety.

Rapid screening of foodborne pathogens has become one of the major challenges to prevent and control the outbreaks of foodborne illnesses (Satija et al., 2016). In recent years, many efforts have been made for simple, rapid and sensitive detection of *E. coli* O157:H7. Yu et al. exploited a fluorescent immunochromatographic strip using CdTe/CdS quantum dots as label for simple and rapid detection of *E. coli* O157:H7 with a low detection limit of $10^4$ CFU/mL (Yu et al., 2017). Jiang et al. developed an immunochromatographic assay using Pt-Au bimetal nanoparticles with peroxidase-like amplification to improve the sensitivity for detection of *E. coli* O157:H7. This reported assay had a low detection limit of $10^2$ CFU/mL with naked eyes (Jiang et al., 2016a). Yu et al. (2018) proposed a quartz crystal microbalance sensor using whole-bacterium SELEX of DNA aptamers for detection of *E. coli* O157:H7, and it could detect *E. coli* O157:H7 as low as $1.46 \times 10^3$ CFU/mL within 50 min. Besides, Guner et al. reported an electrochemical immunosensor for detection of *E. coli* O157:H7 using chitosan, MWCNT, polypyrrole with gold nanoparticles hybrid sensing platform, and it was able to detect *E. coli* O157:H7 ranging from $3 \times 10^1$ to $3 \times 10^7$ CFU/mL (Güner et al., 2017). With fast

* Corresponding author at: Key Laboratory of Agricultural Information Acquisition Technology, Ministry of Agriculture, China Agricultural University, Beijing 100083, China.
*E-mail address:* jianhan@cau.edu.cn (J. Lin).

https://doi.org/10.1016/j.bios.2018.10.006
Received 20 July 2018; Received in revised form 30 September 2018; Accepted 3 October 2018
Available online 11 October 2018
0956-5663/ 

development of nanotechnology, new biosensing methods have emerged for detection of foodborne pathogens. Among them, localized surface plasmon resonance (LSPR) of gold nanoparticles (AuNPs) combined with immunological assays has drawn increasing attentions (Chen et al., 2017a; de la Rica and Stevens, 2013; Kim et al., 2018). AuNP is an excellent signal indicator for biosensor development due to its high extinction coefficient (Chang et al., 2016). The aggregation of the AuNPs can be induced by inter-AuNPs cross linking and result in color change of the AuNPs from red to blue, which can be discriminated easily with naked eyes (Liu et al., 2016; Wu et al., 2016; Zhang et al., 2016a). Recently, some colorimetric biosensors based on AuNP aggregation have been reported for detection of cancer biomarker (Liu et al., 2016), sulfite ion (Du et al., 2012), phenols (Zhang et al., 2016b), H7N9 avian influenza virus (Zhang et al., 2016a) and human prostate specific antigen (Yang and Tseng, 2016) with high sensitivity and wide linear range.

In the past decade, some facile electronic platforms, such as smart phones and pads, have become more and more popular in the development of low-cost, portable and rapid biosensors (Chen et al., 2017b; Guo et al., 2018; Li et al., 2018). With high-speed processor, high-resolution camera and ubiquitous wireless communication, smart phones with tailored APPs have been often used for image collection or data analysis and reported for in-field detection of salivary cortisol (Zangheri et al., 2015), norovirus (Cho et al., 2017), bacteria (Zangheri et al., 2015; Zeinhom et al., 2018a; Zhang and Liu, 2016). Besides, smart phones are often functionalized with global positioning system, and can indicate accurate location for sample collection on the preloaded electronic map. Moreover, microfluidic chips have been frequently reported for rapid detection of foodborne pathogens due to their precise control of fluids, reduced consumption of samples and reagents, shortened detection time and miniaturized analytical platform (Cai et al., 2016; Goluch et al., 2009; Xiong et al., 2018). Therefore, the combination of smart phone, microfluidic chip and immunoassay might be possible to provide simple and low-cost platforms for rapid screening of foodborne pathogens.

In this study, we intended to develop a novel microfluidic biosensor based on gold nanoparticle aggregation and smart phone imaging for simple, rapid and sensitive detection of *E. coli* O157:H7 in chicken samples. As shown in Scheme 1, this proposed biosensor was based on the HRP + $H_2O_2$ + tyramine (TYR) system. The magnetic nanoparticles (MNPs) modified with the capture antibodies (CAbs) against *E. coli* O157:H7 and the polystyrene microspheres (PSs) modified with the detection antibodies (DAbs) against *E. coli* O157:H7 and the catalases were first mixed with the sample containing the target *E. coli* O157:H7 cells in the first mixing channel of the microfluidic chip, and the MNP-bacteria-PS complexes were then formed and captured in the separation chamber by the external magnetic field. After hydrogen peroxide was injected and catalyzed by the catalases on the complexes, the mixture of the AuNPs and the crosslinking agents was injected to react with the catalysate in the second mixing channel and incubated in the detection chamber. The aggregation of the AuNPs was triggered through the crosslinking of phenolic hydroxyl moieties in TYR by the C–C and C–O couplings between aromatic rings (Bui et al., 2015; Chen and Park, 2017b; Liang et al., 2018), and resulted in the color of the AuNPs changing from blue to red. Finally, the color change was detected using the Hue-Saturation-Lightness (HSL)-based imaging APP on the Android smart phone and used to determine the concentration of the target bacteria.

## 2. Materials and methods

### 2.1. Materials

*E. coli* O157:H7 (ATCC 43888) was used as target bacteria, and *Listeria monocytogenes* (ATCC 13932) and *Salmonella typhimurium* (ATCC14028) were used as non-target bacteria. The biotinylated polyclonal CAbs (4–5 mg/mL) against *E. coli* O157:H7 purchased from Meridian (Cincinnati, OH, US) and the monoclonal Dabs (1.25 mg/mL) against *E. coli* O157:H7 obtained from Nanchang University were used for immunological reaction with *E. coli* O157:H7. Gold (III) chloride trihydrate ($HAuCl_4$) from Sigma Aldrich (St. Louis, MO, US) and trisodium citrate from Aladdin (Shanghai, China) were used for the synthesis of the AuNPs. The streptavidin-modified magnetic nanoparticles (~1 mg/mL) with the diameter of ~150 nm obtained from Ocean Nano (MHS-150–10, Dunedin, FL, US) were used for immunomagnetic separation of *E. coli* O157:H7. The carboxyl-modified polystyrene microspheres (~50 mg/mL) with the diameter of 1 μm were obtained from Bangs laboratories (PS04001, IN, US). N-(3-

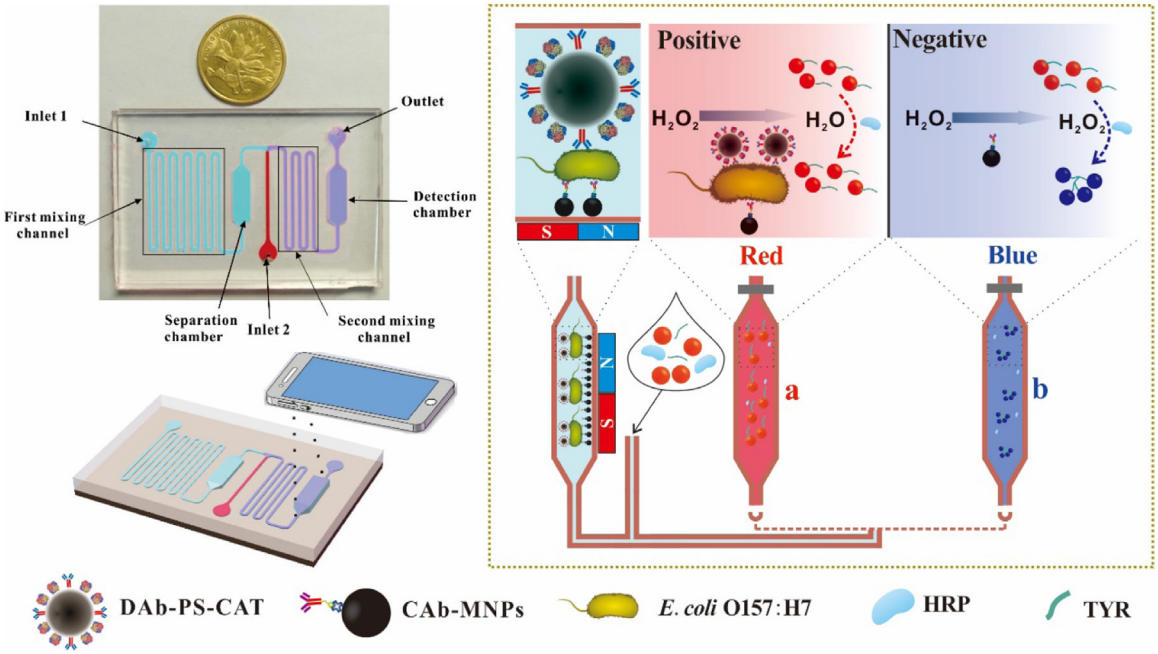


**Scheme 1.** The principle of the proposed colorimetric biosensor for rapid detection of *Escherichia coli* O157:H7 based on gold nanoparticle aggregation and smart phone imaging.

dimethylaminopropyl)-N′-ethylcarbodiimide hydrochloride (EDC·HCl) was used for coupling the DAbs to the PSs carrier. Bovine liver catalase (CAT) from Sigma Aldrich was used for catalyzing hydrogen peroxide to trigger the aggregation of the AuNPs. Bovine serum albumin (BSA) from Sigma Aldrich was used for blocking. Hydrogen peroxide ($H_2O_2$), tyramine and horseradish peroxidase (HRP) from Aladdin (Shanghai, China) were used as the crosslinking agents. Brain heart infusion (BHI) medium from Remel (Lenexa, KS, US) and Luria-Bertani (LB) medium (Aoboxing Biotech, Beijing, China) were used for bacteria culture. The silicone elastomer kit (Sylgard 184) from Dow Corning was used to fabricate the poly(dimethoxy)silane (PDMS) channel. The Objet24 3D printer from Stratasys (Eden Prairie, MN, US) was used to fabricate the mold of the channel. The glass slide from Sail Brand (7101, Jinan, China) was used to bond with the PDMS channel to develop the microfluidic chip. The deionized water was produced by Millipore Advantage 10 (18.2 MΩ cm, Billerica, MA, US) and used for preparing all the solutions. Other reagents were of analytical grade and obtained from Beijing Chemical Reagents (Beijing, China).

### 2.2. Preparation of the bacteria

The bacterial cultures, which were stored at −20 °C as glycerol stock, were revived and grown in BHI broth overnight at 37 °C for activation. After the bacteria were cultured in 5 mL of LB at 37 °C for 12–16 h with shaking at 180 rpm respectively, they were serially 10-fold diluted with the sterile PBS to the final concentrations from $5.0 \times 10^1$ to $5.0 \times 10^8$ CFU/mL. The prepared bacteria were inactivated by boiling at 90 °C for 10 min and stored at 4 °C for further use.

For bacterial enumeration, the bacteria were serially 10-fold diluted with the sterile PBS and 100 μL of the diluents were surface plated on the LB agar plates. The plates were incubated at 37 °C for 22–24 h and the visible colonies were counted for the enumeration of the bacteria.

### 2.3. Design and fabrication of the microfluidic chip

The microfluidic chip is the key component of this proposed biosensor. It consisted of three parts: (1) two serpentine mixing channels with the width of 600 μm and the height of 100 μm for mixing the bacterial sample with the mixture of the MNPs and the PSs in the first mixing channel and mixing the catalysate with the mixture of the AuNPs and the cross-linking agents in the second one, (2) the separation chamber with the length of 14 mm, the width of 4 mm and the height of 1 mm for separating the MNP-bacteria-PS complexes and catalyzing hydrogen peroxide, and (3) the detection chamber with the length of 14 mm, the width of 4 mm and the height of 2 mm for monitoring the color change of the AuNPs.

The microfluidic chip was fabricated based on 3D printing and surface plasma bonding. As shown in Scheme 1, the 3D drawing in. stl format was first designed using the Solidworks software, and the mold was printed using the Objet24 3D printer. Prior to use, the mold was immersed in 5% NaOH for 30 min to thoroughly remove the surplus support material. The prepolymer of PDMS was then mixed with the curing agent at the ratio of 10:1. After degassing for 20 min in vacuum, the mixture was poured into the mold and cured at 65 °C for 12 h. Finally, the PDMS replica was peeled off and bonded onto the glass slide to form the microfluidic chip after surface plasmon treatment (Harrick Plasma, Ithaca, NY, US).

### 2.4. Synthesis of the AuNPs

The previously reported hydrothermal reduction method was used to synthesize the AuNPs based on the reduction of $HAuCl_4$ with tri-sodium citrate in water at boiling point (Li et al., 2014a, 2014b). Briefly, 25 mL of 38.8 mM tri-sodium citrate was first added into 250 mL of the boiling $HAuCl_4$ solution (1 mM). Then, the mixture was quickly stirred and heated, until its color changed from light yellow to dark red. After cooling to room temperature, the absorbance of the AuNPs was measured and the concentration of the AuNPs was determined as approximately 19 nM according to Beer's law (Yuan et al., 2015).

### 2.5. Preparation of the DAb-PS-CAT conjugates

First, 40 μL of the carboxylated PSs (50 mg/mL) were transferred into a centrifuge tube containing 1 mL of PB (pH 6.0, 0.01 M) and centrifuged at 7000 rpm for 10 min to remove the supernatant. Then, 25 mL of PB was used to resuspend the PSs in the conical flask, followed by successive adding of 0.08 mg of the detection antibodies and 0.5 mg of the catalases. After the mixture was gently stirred at room temperature for 1 h, 150 μL of EDC (1 mg/mL) was added into the mixture and incubated for 1 h with gentle mixing. Besides, 200 μL of 10% BSA (w/v) and 200 μL of EDC were added and incubated for another 60 min to minimize non-specific binding. Finally, the mixture were centrifuged and the precipitates were resuspended with 1 mL of PBS containing 1% BSA to obtain the DAb-PS-CAT conjugates, which were stored at 4 °C for further use.

### 2.6. Separation and detection of E. coli O157:H7

The separation and detection of *E. coli* O157:H7 were based on immunomagnetic separation of the target bacteria in the separation chamber and colorimetric measurement of the aggregated AuNPs in the detection chamber, respectively. Prior to test, 20 μg of the CAb-modified MNPs and 25 μg of the DAb and CAT modified PSs were completely mixed. The mixture of the MNPs and the PSs was first injected together with 50 μL of *E. coli* O157:H7 ($5.0 \times 10^1$–$5.0 \times 10^8$ CFU/mL) at the flow rate of 50 μL/min using the precise syringe pumps (Pump 11 elite, Harvard Apparatus, Holliston, MA, US) into the first mixing channel and collected in the separation chamber. After incubation for 10 min to form the MNP-bacteria-PS-CAT complexes, the external magnetic field was applied to capture the complexes against the glass bottom of the chamber, followed by washing with PBST at the flow rate of 50 μL/min for 10 min to remove the unbound PSs. Then, 50 μL of $H_2O_2$ (0.5 mM) was injected into the chamber and catalyzed by the CAT on the complexes for 20 min. The catalysate and the cross-linking agents containing 20 μL of HRP (20 μg/mL), 5 μL of TYR (2 mM) and 50 μL of the AuNPs (~19 nM) were simultaneously injected into the second mixing channel and collected in the detection chamber. The color of the AuNPs in the detection chamber was collected and analyzed using the imaging APP on the smart phone after 5 min to determine the concentration of the target bacteria.

### 2.7. Detection of E. coli O157:H7 in the spiked chicken samples

The chicken samples were purchased from the local supermarket. According to the food safety national standards, 25 g of the chicken sample was first added into 225 mL of PBS and homogenized for 4 min using the stomacher (BagMixer CC, InterScience, Paris, France). Then, different concentrations of *E. coli* O157:H7 were added into the supernatant to prepare the spiked chicken samples with the bacterial concentration of $5.0 \times 10^0$ - $5.0 \times 10^4$ CFU/mL. Finally, the spiked samples were detected using the proposed biosensor according to the protocol in Section 2.6.

## 3. Results and discussion

### 3.1. Simulation on the mixing channels in the microfluidic chip

The mixing efficiency of the microfluidic chip has great impact on the detection time and the sensitivity of the proposed biosensor. The mixing of the fluids in the microfluidic channels mainly depends on the

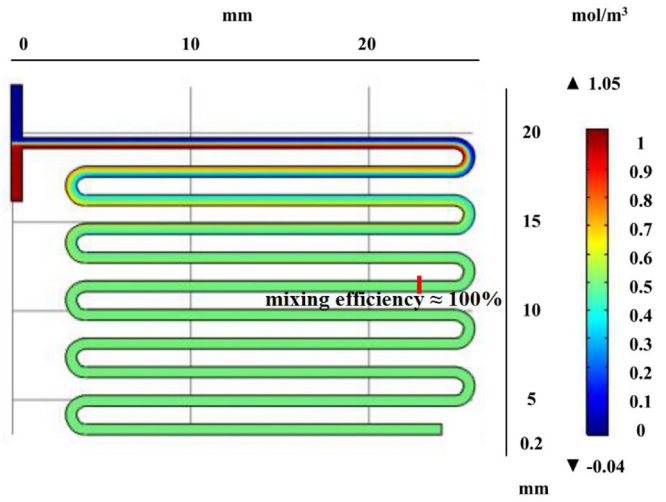


**Fig. 1.** The simulation on mixing efficiency of the serpentine microfluidic mixing channels.

diffusion, and generally requires a certain distance to achieve complete mixing. More importantly, the separation and detection of the target bacteria are based on the immunoreaction between the antibodies and the target bacteria, which also requires a certain time to achieve stable conjugation. Therefore, COMSOL was used to simulate the serpentine mixing channels based on free triangular grid and finite volume, and the results were shown in Fig. 1. The mixing efficiency was up to 82.5% when the length increased from 0 mm to 45 mm, and almost reached 100% when the length increased to 100 mm. This indicated that the serpentine mixing channel with the length of 100 mm was sufficient for complete mixing of the sample and the mixture of the MNPs and the PSs. To ensure the forming of the MNP-bacteria-PS complexes, the length was doubled in the design of these two mixing channels, allowing sufficient immunoreaction and conjugation.

### 3.2. Confirmation of the aggregation of the AuNPs

This proposed biosensor was based on the aggregation of the AuNPs stimulated by hydroxyl radical through the crosslinking of phenolic hydroxyl moieties in TYR by the C–C and C–O couplings between aromatic rings. To verify the aggregation of the AuNPs, the tests on coloration reaction of the AuNPs and the crosslinking agents including $H_2O_2$, HRP and TYR were conducted. As shown in Fig. 2a, the color change from red to blue only occurred when $H_2O_2$, HRP, TYR and the AuNPs were all present, and the color remained red when either $H_2O_2$, or HRP, or TYR was absent. The color change could be read with naked eyes. To analyze the color change, the imaging APP was developed and loaded on the Android smart phone (STF-AL10, Resolution: 1920 × 1080 pixels, Huawei, Shenzhen, China) to monitor the color change, and the Hue-Saturation-Lightness (HSL) color space was used for the image processing instead of the conventional Red-Green-Blue one. As shown in Fig. 2b, the hue of the mixture of $H_2O_2$, HRP, TYR and the AuNPs was obviously less than those of all other mixtures, indicating that only the presence of $H_2O_2$, HRP and TYR could stimulate the aggregation of the AuNPs.

To confirm the aggregation of the AuNPs, transmission electron microscopy (TEM) and dynamic light scattering (DLS) were used to characterize the AuNPs before and after aggregation. The TEM images were shown in Fig. 2c-d, and it could be seen that the AuNPs had an average diameter of 13 nm before aggregation and were dramatically enlarged to ~670 nm after aggregation, which were also confirmed by DLS analysis (Fig. S1a). To further analyze the color change, the aggregation of the AuNPs was monitored using the UV–VIS spectrophotometer (Shimadzu, UV-2300, Japan) and the spectra showed that the AuNPs had an absorption peak at 520 nm and the aggregated AuNPs had another peak at 630 nm (Fig. S1b). This also confirmed the aggregation of the AuNPs.

### 3.3. Optimization of the proposed biosensor

The capture antibodies modified magnetic nanoparticles and the detection antibodies and the catalases modified polystyrene microspheres play important roles in the development of this proposed biosensor. The amount of the MNPs was optimized and reported in our previous studies (Chen et al., 2016), and the optimal amount of 20 μg was used in this study. Different amounts of the PSs were used with the optimal amount of the MNPs for the detection of the target bacteria at the concentration of $3.5 \times 10^3$ CFU/mL to optimize the amount of the PSs. As shown in Fig. S2a, the hue increased quickly from ~238 to ~277 when the amount of the PSs changed from 3 μg to 25 μg, and did

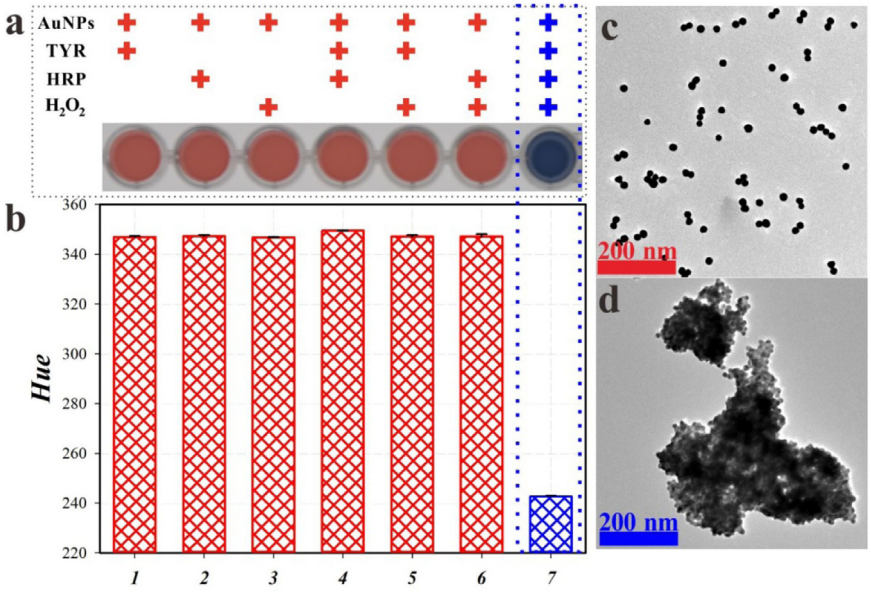


**Fig. 2.** (a) The results on the mixing of the AuNPs with different combinations of the cross-linking agents; (b) The hue of the mixtures of the AuNPs with different combinations of the cross-linking agents; (c) The TEM image of the AuNPs before aggregation; (d) The TEM image of the AuNPs after aggregation.

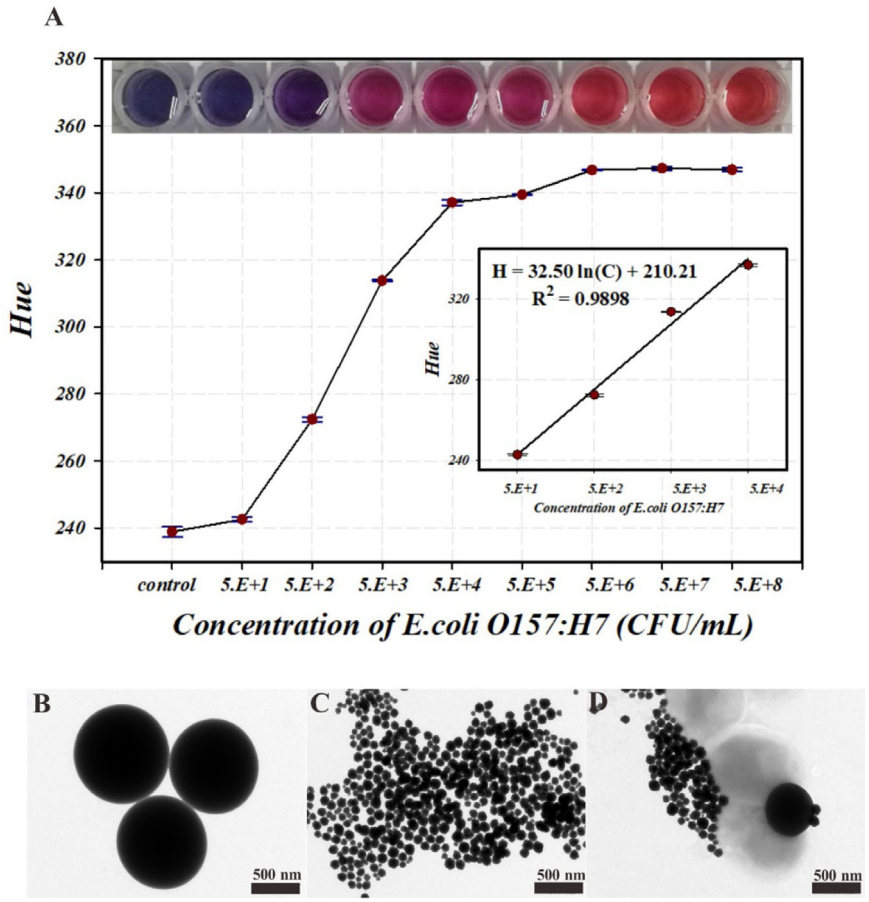


**Fig. 3.** (A) Calibration curve of this proposed biosensor; (B) The TEM image of the PSs; (C) The TEM image of the MNPs; (D) The TEM image of the MNP-bacteria-PS complexes.

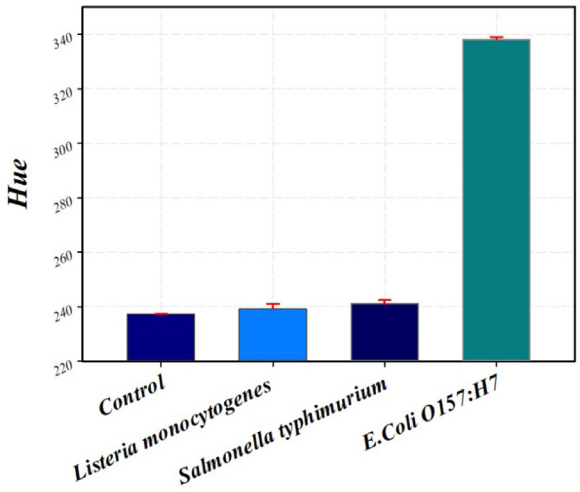


**Fig. 4.** The specificity of the proposed biosensor to the non-target bacteria.

not increased obviously when the amount was 50 μg. It was mentionable that the color of the AuNPs changed from blue to red when the hue was 273 and the amount of the PSs was 25 μg. Therefore, the optimal amount of 25 μg was used in this study.

The concentration of $H_2O_2$ and the time for enzymatic catalysis also have great impact on the sensitivity of the proposed biosensor. To evaluate the effect of $H_2O_2$ on the biosensor, different concentrations of $H_2O_2$ ranging from 0 to 1 mM were used for detection of the target bacteria at the concentration of $3.5 \times 10^3$ CFU/mL. As shown in Fig. S2b, the hue decreased quickly from 356 to 241 when the concentration of $H_2O_2$ increased from 0 to 0.5 mM, and remained stable when the concentration of $H_2O_2$ increased to 1 mM. Thus, the optimal concentration of 0.5 mM was used in this study. Besides, different times for enzymatic catalysis ranging from 5 min to 30 min were used for detection of the target bacteria at the concentration of $3.5 \times 10^3$ CFU/mL. As shown in Fig. S2c, the hue gradually increased from 250 to 338 when the time changed from 5 min to 20 min, and did not increase obviously when the time was 30 min. Therefore, the optimal time of 20 min was used in this study.

### 3.4. Detection of E. coli O157:H7 using the proposed biosensor

Under the optimal conditions, different concentrations of *E. coli* O157:H7 ranging from $5.0 \times 10^1$ CFU/mL to $5.0 \times 10^8$ CFU/mL were detected using this proposed biosensor. As shown in Fig. 3A, the color of the AuNPs obviously changed from blue to violet, then to pink and final to red when the concentration of *E. coli* O157:H7 increased from $5.0 \times 10^1$ CFU/mL to $5.0 \times 10^8$ CFU/mL, which could be distinguished with naked eyes. The color change of the AuNPs was further measured using the HSL color space based smart phone imaging APP to obtain their hue. The hue ($\boldsymbol{H}$) was found to have a good linear relationship with the concentration ($\boldsymbol{C}$) of *E. coli* O157:H7 ranging from $5.0 \times 10^1$ to $5.0 \times 10^4$ CFU/mL, and the calibration curve of this proposed biosensor could be described as $\boldsymbol{H} = 32.50 \ln(\boldsymbol{C}) + 210.21$ ($R^2 = 0.98$). Based on 3 times of signal-to-noise ratio, the low detection limit of this biosensor was calculated to be 50 CFU/mL. Besides, the TEM imaging was used to verify the forming of the PSs, the MNPs and the MNP-bacteria-PS complexes (Fig. 3B–D).

The specificity of this proposed biosensor was evaluated using two

**Table 1**
Detection of *E. coli* O157:H7 in chicken samples using the proposed biosensor.

| Sample | Spiked(CFU/mL) | Hue | Detected(CFU/mL) | Recovery(%) | CV(%) |
|---|---|---|---|---|---|
| 1 | 0 | 238.12 | ND[a] | – | – |
| 2 | 0 | 236.36 | ND | – | – |
| 3 | 50 | 243.01 | 51 | 102.04 | 0.87 |
| 4 | 50 | 242.15 | 48 | 96.08 | 1.26 |
| 5 | 500 | 275.21 | 500 | 100.00 | 0.38 |
| 6 | 500 | 276.73 | 557 | 111.34 | 0.98 |
| 7 | 50,000 | 337.38 | 40,139 | 80.27 | 0.23 |
| 8 | 50,000 | 335.45 | 45,685 | 91.37 | 0.46 |

[a] ND: Not detectable.

common pathogenic bacteria, *Listeria monocytogenes* and *Salmonella typhimurium*. The similar concentration ($2.7 \times 10^4$ CFU/mL) of the target bacteria, these two non-target bacteria, and the negative controls were detected using this proposed biosensor. As shown in Fig. 4, the hue of the target bacteria was much larger than those of these two non-target bacteria, which were close to that of the negative controls. This indicated that this proposed biosensor had a good specificity, and this could be attributed to the good specificity of the capture antibodies and the detection antibodies against *E. coli* O157:H7.

### 3.5. Detection of E. coli O157:H7 in the spiked chicken samples

To further evaluate the applicability of this proposed biosensor for detection of *E. coli* O157:H7 in food samples, eight chicken samples were purchased from the local supermarket and pretreated according to the food safety national standards. Briefly, 25 g of each chicken meat was added into 225 mL of PBS and was homogenized for 4 min. After standing for 5 min, the supernatant was collected and different concentrations of the target bacteria were spiked into the supernatant, followed by bacteria separation and detection using this proposed biosensor under the optimal conditions. As shown in Table 1, the recoveries for different concentrations ($5.0 \times 10^1$–$5.0 \times 10^4$ CFU/mL) of *E. coli* O157:H7 in chicken samples ranged from 80.27% to 111.34%, and the average recovery was 96.83%, indicating that the proposed biosensor was applicable for detection of *E. coli* O157:H7 in food samples.

## 4. Conclusions

In summary, we have successfully developed a microfluidic biosensor based on gold nanoparticle aggregation and smart phone imaging for rapid and sensitive detection of *E. coli* O157:H7. Under the optimal conditions, this biosensor was able to detect *E. coli* O157:H7 as low as 50 CFU/mL within 1 h. The proposed biosensor has shown the merits of simple device for data processing, high integration for sample and reagent handling, low cost for microfluidic chip fabrication, and small size for in-field application. However, the immune reaction efficiency was not very satisfied, and might be improved using smaller-sized passive mixers or active micromixers to further reduce the detection time. Although this proposed biosensor currently was still not able to meet the demand on the detection limit of 1 CFU/mL for practical applications in food safety, it would be combined with continuous-flow immunomagnetic separation of the target bacteria from larger volume of food sample to further improve the sensitivity in the future.

## Acknowledgments

This study was supported in part by the National Key Research and Development of China, China (2016YFD0201201), Walmart Foundation, United States (SA17031161) and Walmart Food Safety Collaboration Center, China. The authors would like to thank Dr. Weihua Lai at Nanchang University for providing the monoclonal antibodies against *E. coli* O157:H7.

## Appendix A. Supporting information

Supplementary data associated with this article can be found in the online version at doi:10.1016/j.bios.2018.10.006.

## References

Bui, M.P., Ahmed, S., Abbas, A., 2015. Single-digit pathogen and attomolar detection with the naked eye using liposome-amplified plasmonic immunoassay. Nano Lett. 15 (9), 6239–6246.
Cai, Z., Xiang, J., Chen, H., Wang, W., 2016. A rapid micromixer for centrifugal microfluidic platforms. Micromachines 7 (5), 89.
Chang, C.C., Chen, C.P., Chen, C.Y., Lin, C.W., 2016. DNA base-stacking assay utilizing catalytic hairpin assembly-induced gold nanoparticle aggregation for colorimetric protein sensing. Chem. Commun. 52 (22), 4167–4170.
Chen, J., Park, B., 2017a. Label-free screening of foodborne Salmonella using surface plasmon resonance imaging. Anal. Bioanal. Chem.
Chen, J., Park, B., 2017b. Label-free screening of foodborne Salmonella using surface plasmon resonance imaging. Anal. Bioanal. Chem.
Chen, Q., Wang, D., Cai, G., Xiong, Y., Li, Y., Wang, M., Huo, H., Lin, J., 2016. Fast and sensitive detection of foodborne pathogen using electrochemical impedance analysis, urease catalysis and microfluidics. Biosens. Bioelectron. 86, 770–776.
Chen, Y., Xianyu, Y., Jiang, X., 2017a. Surface modification of gold nanoparticles with small molecules for biochemical analysis. Acc. Chem. Res. 50 (2), 310–319.
Chen, Y., Xianyu, Y., Wu, J., Dong, M., Zheng, W., Sun, J., Jiang, X., 2017b. Double-enzymes-mediated bioluminescent sensor for quantitative and ultrasensitive point-of-care testing. Anal. Chem. 89 (10), 5422–5427.
Cho, S., Park, T.S., Reynolds, K.A., Yoon, J.-Y., 2017. Multi-normalization and interpolation protocol to improve norovirus immunoagglutination assay from paper microfluidics with smartphone detection. SLAS Technol. 22 (6), 609–615.
de la Rica, R., Stevens, M.M., 2013. Plasmonic ELISA for the detection of analytes at ultralow concentrations with the naked eye. Nat. Protoc. 8 (9), 1759–1764.
Du, J., Shao, Q., Yin, S., Jiang, L., Ma, J., Chen, X., 2012. Colorimetric chemodosimeter based on diazonium-gold-nanoparticle complexes for sulfite ion detection in solution. Small 8 (22), 3412–3416.
Feng, M., Yong, Q., Wang, W., Kuang, H., Wang, L., Xu, C., 2013. Development of a monoclonal antibody-based ELISA to detect Escherichia coli O157:H7. Food Agric. Immunol. 24 (4), 481–487.
Goluch, E.D., Stoeva, S.I., Lee, J.S., Shaikh, K.A., Mirkin, C.A., Liu, C., 2009. A microfluidic detection system based upon a surface immobilized biobarcode assay. Biosens. Bioelectron. 24 (8), 2397–2403.
Güner, A., Çevik, E., Şenel, M., Alpsoy, L., 2017. An electrochemical immunosensor for sensitive detection of Escherichia coli O157:H7 by using chitosan, MWCNT, polypyrrole with gold nanoparticles hybrid sensing platform. Food Chem. 229, 358–365.
Guo, L., Shi, Y., Liu, X., Han, Z., Zhao, Z., Chen, Y., Xie, W., Li, X., 2018. Enhanced fluorescence detection of proteins using ZnO nanowires integrated inside microfluidic chips. Biosens. Bioelectron. 99, 368–374.
Jiang, T., Song, Y., Wei, T., Li, H., Du, D., Zhu, M.-J., Lin, Y., 2016a. Sensitive detection of Escherichia coli O157:H7 using Pt–Au bimetal nanoparticles with peroxidase-like amplification. Biosens. Bioelectron. 77, 687–694.
Jiang, T., Song, Y., Wei, T., Li, H., Du, D., Zhu, M.J., Lin, Y., 2016b. Sensitive detection of Escherichia coli O157:H7 using Pt-Au bimetal nanoparticles with peroxidase-like amplification. Biosens. Bioelectron. 77, 687–694.
Kim, J., Oh, S.Y., Shukla, S., Hong, S.B., Heo, N.S., Bajpai, V.K., Chun, H.S., Jo, C.H., Choi, B.G., Huh, Y.S., 2018. Heteroassembled gold nanoparticles with sandwich-immunoassay LSPR chip format for rapid and sensitive detection of hepatitis B virus surface antigen (HBsAg). Biosens. Bioelectron. 107, 118–122.
King, T., Cole, M., Farber, J.M., Eisenbrand, G., Zabaras, D., Fox, E.M., Hill, J.P., 2017. Food safety for food security: Relationship between global megatrends and developments in food safety. Trends Food Sci. Technol.
Li, F., Li, H., Wang, Z., Wu, J., Wang, W., Zhou, L., Xiao, Q., Pu, Q., 2018. Mobile phone mediated point-of-care testing of HIV p24 antigen through plastic micro-pit array chips. Sens. Actuators B: Chem. 271 (189–194).
Li, N., Zhao, P., Astruc, D., 2014a. Anisotropic gold nanoparticles: synthesis, properties, applications, and toxicity. Angew. Chem. 53 (7), 1756–1789.
Li, Y., Tang, Z., Prasad, P.N., Knecht, M.R., Swihart, M.T., 2014b. Peptide-mediated synthesis of gold nanoparticles: effects of peptide sequence and nature of binding on physicochemical properties. Nanoscale 6 (6), 3165–3172.
Liang, Y., Huang, X., Chen, X., Zhang, W., Ping, G., Xiong, Y., 2018. Plasmonic ELISA for naked-eye detection of ochratoxin A based on the tyramine-H2O2 amplification system. Sens. Actuators B Chem. 259, 162–169.
Liu, H., Rong, P., Jia, H., Yang, J., Dong, B., Dong, Q., Yang, C., Hu, P., Wang, W., Liu, H., Liu, D., 2016. A Wash-free homogeneous colorimetric immunoassay method. Theranostics 6 (1), 54–64.
Omari, R., Frempong, G.K., Arthur, W., 2018. Public perceptions and worry about food safety hazards and risks in Ghana. Food Control.
Satija, J., Punjabi, N., Mishra, D., Mukherji, S., 2016. Plasmonic-ELISA: expanding horizons. RSC Adv. 6 (88), 85440–85456.

Wu, S., Tan, S.Y., Ang, C.Y., Luo, Z., Zhao, Y., 2016. Oxidation-triggered aggregation of gold nanoparticles for naked-eye detection of hydrogen peroxide. Chem. Commun. 52 (17), 3508–3511.
Wu, X., Wang, W., Liu, L., Kuang, H., Xu, C., 2015. Monoclonal antibody-based cross-reactive sandwich ELISA for the detection of Salmonella spp. in milk samples. analytical. Methods 7 (21), 9047–9053.
Xiong, Q., Lim, C.Y., Ren, J., Zhou, J., Pu, K., Chan-Park, M.B., Mao, H., Lam, Y.C., Duan, H., 2018. Magnetic nanochain integrated microfluidic biochips. Nat. Commun. 9 (1), 1743.
Yang, Y.C., Tseng, W.L., 2016. 1,4-Benzenediboronic-acid-induced aggregation of gold nanoparticles: application to hydrogen peroxide detection and biotin-avidin-mediated immunoassay with naked-eye detection. Anal. Chem. 88 (10), 5355–5362.
Yu, J., Su, J., Zhang, J., Wei, X., Guo, A., 2017. CdTe/CdS quantum dot-labeled fluorescent immunochromatography test strips for rapid detection of Escherichia coli O157:H7. Rsc Adv. 7 (29), 17819–17823.
Yu, X., Chen, F., Wang, R., Li, Y., 2018. Whole-bacterium SELEX of DNA aptamers for rapid detection of E.coli O157:H7 using a QCM sensor. J. Biotechnol. 266, 39–49.
Yuan, Z., Lu, F., Peng, M., Wang, C.W., Tseng, Y.T., Du, Y., Cai, N., Lien, C.W., Chang, H.T., He, Y., Yeung, E.S., 2015. Selective colorimetric detection of hydrogen sulfide based on primary amine-active ester cross-linking of gold nanoparticles. Anal. Chem. 87 (14), 7267–7273.
Zangheri, M., Cevenini, L., Anfossi, L., Baggiani, C., Simoni, P., Di Nardo, F., Roda, A., 2015. A simple and compact smartphone accessory for quantitative chemiluminescence-based lateral flow immunoassay for salivary cortisol detection. Biosens. Bioelectron. 64, 63–68.
Zeinhom, M.M.A., Wang, Y., Sheng, L., Du, D., Li, L., Zhu, M.-J., Lin, Y., 2018a. Smart phone based immunosensor coupled with nanoflower signal amplification for rapid detection of Salmonella Enteritidis in milk, cheese and water. Sens. Actuators B: Chem. 261, 75–82.
Zeinhom, M.M.A., Wang, Y., Song, Y., Zhu, M.J., Lin, Y., Du, D., 2018b. A portable smartphone device for rapid and sensitive detection of E. coli O157:H7 in yoghurt and egg. Biosens. Bioelectron. 99, 479–485.
Zhang, D., Liu, Q., 2016. Biosensors and bioelectronics on smartphone for portable biochemical detection. Biosens. Bioelectron. 75, 273–284.
Zhang, H., Ma, X., Hu, S., Lin, Y., Guo, L., Qiu, B., Lin, Z., Chen, G., 2016a. Highly sensitive visual detection of avian influenza A (H7N9) virus based on the enzyme-induced metallization. Biosens. Bioelectron. 79, 874–880.
Zhang, L.-p., Xing, Y.-p., Liu, L.-h., Zhou, X.-h., Shi, H.-c., 2016b. Fenton reaction-triggered colorimetric detection of phenols in water samples using unmodified gold nanoparticles. Sens. Actuators B: Chem. 225, 593–599.